

Vibrational vs. electronic coherences in 2D spectrum of molecular systems

Vytautas Butkus,^{1,2} Donatas Zigmantas,³ Leonas Valkunas,^{1,2} and Darius Abramavicius^{1,4, a)}

¹⁾*Department of Theoretical Physics, Faculty of Physics, Vilnius University, Sauletekio 9-III, LT-10222 Vilnius, Lithuania*

²⁾*Center for Physical Sciences and Technology, Gostauto 9, LT-01108 Vilnius, Lithuania*

³⁾*Department of Chemical Physics, Lund University, P.O. Box 124, 22100 Lund, Sweden*

⁴⁾*State Key Laboratory of Supramolecular Complexes, Jilin University, 2699 Qianjin Street, Changchun 130012, PR China*

Two-dimensional spectroscopy has recently revealed the oscillatory behavior of the excitation dynamics of molecular systems. However, in the majority of cases there is considerable debate over what is actually being observed: excitonic or vibrational wavepacket motion or evidence of quantum transport. In this letter we present a method for distinguishing between vibrational and excitonic wavepacket motion, based on the phase and amplitude relationships of oscillations of distinct peaks as revealed through a fundamental analysis of the two-dimensional spectra of two representative systems.

Two-dimensional photon-echo (2DPE) spectroscopy is a powerful tool capable of resolving quantum correlations on the femtosecond timescale¹⁻³. They appear as beats of specific peaks in the 2DPE spectrum for a number of molecular systems^{3,4}. However, the underlying processes are often ambiguous. At first, the beats were attributed to the wave-like quantum transport with quantum coherences being responsible for an ultra-efficient excitation transfer³⁻⁶. The same process was associated with the opposite phase beats in the spectral regions which are symmetric with respect to the diagonal line⁷.

In molecules and their aggregates, electronic transitions are coupled to various intra- and intermolecular vibrational modes. Vibrational energies of these are of the order of 100 - 3000 cm^{-1} , while the magnitudes of the resonant couplings, J , in excitonic aggregates (e.g. in photosynthetic pigment-protein complexes or in J-aggregates) are in the same range. Thus, vibronic and excitonic systems show considerable spectroscopic similarities, and presence of electronic and/or vibrational beats in the 2DPE spectrum is expected. Indeed, similar spectral beats originating entirely from a high-energy vibrational wavepacket motion have been observed^{8,9}. The possibility of distinguishing the electronic and vibrational origin of the beats from a 2DPE spectrum has been emphasized in a recent letter¹⁰. However, the reported conclusions have not been supported by theoretical arguments, and thus are questionable. Therefore, the highly relevant question of how vibrations interfere with electronic coherences in 2DPE spectrum is still an open one. A theoretical study of the origin of spectral beats, their phase relationships in the rephasing and non-rephasing components of the 2DPE spectrum is presented in this article.

We address this problem by considering two generic model systems which exhibit distinct internal coherent dynamics. The simplest model of an isolated molecular electronic excitation is the vibronic system represented

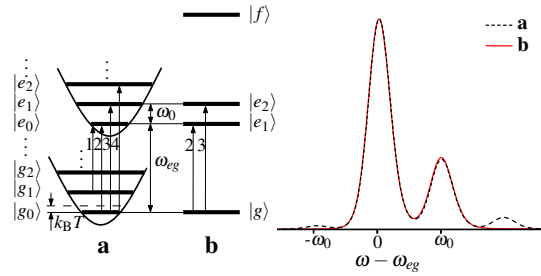


FIG. 1. Energy level structure of the displaced oscillator (a) and electronic dimer (b) and corresponding linear absorption spectra.

by two electronic states, $|g\rangle$ and $|e\rangle$, which are coupled to a one-dimensional nuclear coordinate q . We denote the model by a *displaced oscillator* (DO) system (Fig. 1a). Taking $\hbar = 1$, the vibronic potential energy surface of the $|e\rangle$ state is shifted up by electronic energy ω_{eg} and its minimum is shifted by d with respect to the ground state $|g\rangle$; d is the dimensionless displacement. This setup results in two vibrational ladders of quantum sub-states $|g_m\rangle$ and $|e_n\rangle$, $m, n = 0 \dots \infty$, characterized by the Huang-Rhys (HR) factor $HR = d^2/2$ ^{11,12}.

The other model system, which shows similar spectroscopic properties but has completely different coherent internal dynamics without vibrations, is an *excitonic dimer* (ED). It consists of two two-level chromophores (sites) with identical transition energies ϵ . The two sites are coupled by the inter-site resonance coupling J . As a result, the ED has one ground state $|g\rangle$, two single-exciton states $|e_1\rangle$ and $|e_2\rangle$ with energies $\epsilon_{e_1, e_2} = \epsilon \pm J$, respectively, and a single double-exciton state $|f\rangle$ with energy $\epsilon_f = 2\epsilon - \Delta$, where Δ is the bi-exciton binding energy (Fig. 1b)¹³.

The absorption spectrum of both systems is as follows. The absorption of the DO is determined by transitions from the $|g_m\rangle$ vibrational ladder into $|e_n\rangle$ scaled by the Franck-Condon (FC) vibrational wavefunction overlaps^{11,13}. Choosing $HR = 0.3$ and $k_B T \approx \frac{1}{3}\omega_0$ and

^{a)}Electronic mail: darius.abramavicius@ff.vu.lt

assuming Lorentzian lineshapes with linewidth γ , we get the vibrational progression in the absorption spectrum (dashed line in Fig. 1). Here ω_0 is the vibrational energy. The most intensive peaks at ω_{eg} and $\omega_{eg} + \omega_0$ correspond to 0-0 and 0-1 vibronic transitions. Qualitatively similar peak structure is featured in the absorption of ED, where the spectrum shows two optical transitions $|g\rangle \rightarrow |e_1\rangle$ and $|g\rangle \rightarrow |e_2\rangle$, assuming both are allowed. Choosing $J = \omega_0/2$ and the angle φ between the chromophore transition dipoles equal to $\pi/6$, and using adequate linewidth parameters, we get absorption peaks (solid line in Fig. 1) that exactly match the strongest peaks of the DO. As expected one cannot distinguish between these two internally different systems from the absorption spectra alone.

The 2DPE spectrum carries more information than absorption. However, it consists of many contributions and unambiguous distinction between the ED and DO systems becomes difficult. In order to unravel the 2DPE spectra we thus need to construct the entire 2D signal from the first principles for both systems and recover the source of oscillations in the 2DPE spectrum.

In the conventional scheme of the 2DPE measurement, two primary excitation pulses with wavevectors \mathbf{k}_1 and \mathbf{k}_2 followed by the probe pulse \mathbf{k}_3 are used; \mathbf{k}_j are pulse wavevectors. The signal is detected at the $\mathbf{k}_S = -\mathbf{k}_1 + \mathbf{k}_2 + \mathbf{k}_3$ phase-matching direction. The order of \mathbf{k}_1 and \mathbf{k}_2 defines the rephasing configuration (\mathbf{k}_I) when \mathbf{k}_1 comes first and the non-rephasing configuration (\mathbf{k}_{II}) when \mathbf{k}_2 comes first.

Semiclassical perturbation theory with respect to the incoming fields reveals the system-field interaction and evolution sequences, often denoted by the Liouville space equations. Three types of distinct interaction configurations are denoted by the Excited State Emission (ESE), Ground State Bleaching (GSB) and Excited State Absorption (ESA) contributions^{12,14}. If we neglect environment-induced relaxation, the signals are given as sums of resonant contributions, $S(\omega_3, t_2, \omega_1) = \sum_n S_n(\omega_3, t_2, \omega_1)$ of the type

$$S_n(\omega_3, t_2, \omega_1) = A_{(n)} \iint dt_1 dt_3 e^{+i\omega_3 t_3 + i\omega_1 t_1} \times [\pm G_3(t_3) G_2(t_2) G_1(t_1)]_{(n)}, \quad (1)$$

where the subscript n denotes different terms of the summation. $A_{(n)}$ is a complex prefactor, given by the transition dipoles and excitation fields, the propagator of the density matrix G for the j th ($j = 1, 2, 3$) time delay is of the one-sided exponential function type

$$G_j(t_j) = \theta(t_j) \exp(-i\varepsilon_j t_j) \quad (2)$$

($\theta(t)$ is the Heaviside step-function). Here ε_j coincides with the energy gap ω_{ab} between the *left* and *right* states of the system density matrix relevant to the time interval t_j . ESE and GSB carry ‘+’ sign while ESA has ‘-’ overall sign.

The Fourier transforms in Eq. (1) map the contributions to the frequency-frequency plot (t_1, t_3) \rightarrow

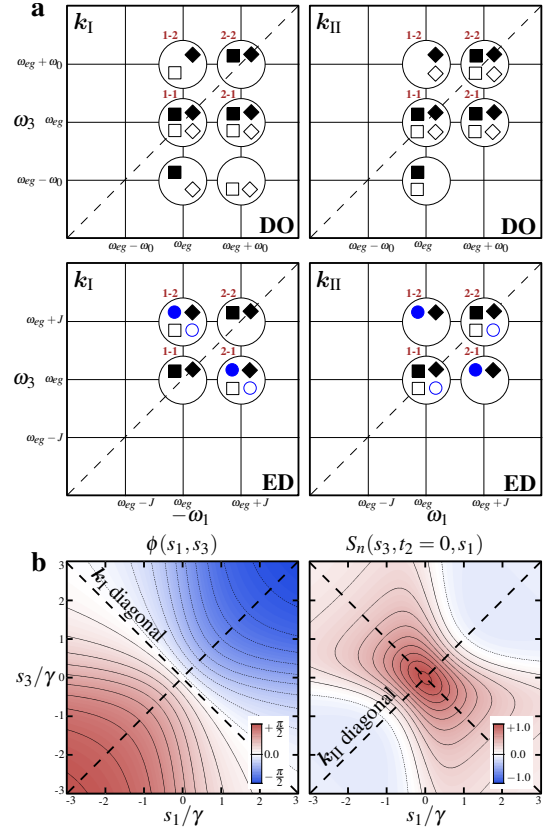


FIG. 2. (a) Scheme of contributions to 2DPE spectrum of the \mathbf{k}_I and \mathbf{k}_{II} signals for the reduced DO and ED ($\Delta = 0$) systems. The ESE contribution is indicated by squares, GSB – diamonds, ESA – circles. Solid symbols denote non-oscillatory contributions in t_2 , open – oscillatory in the form of $\pm \cos(\varepsilon_2 t_2)$, where $\varepsilon_2 = \omega_0$ for DO and $\varepsilon_2 = 2J$ for ED. (b) Phase ϕ of the contribution (Eq. 3) and peak profile S_n as a function of the shift from the peak center ($s_1 = s_3 = 0$) using relative coordinates. The diagonal lines of the \mathbf{k}_I and \mathbf{k}_{II} contributions to the 2D spectra are shown by dashed lines. Peaks are labeled in plots as ‘1-1’, ‘1-2’, etc.

(ω_1, ω_3) \sim ($\mp|\varepsilon_1|, \varepsilon_3$) (the upper sign is for \mathbf{k}_I , the lower – for \mathbf{k}_{II}). Diagonal peaks at $\omega_1 = \mp\omega_3$ are usually distinguished, while the anti-diagonal line is defined as $\mp\omega_1 + \omega_3 = Const$. The whole 2DPE signal becomes a function of t_2 : either oscillatory for density matrix coherences $|a\rangle\langle b|$ with characteristic oscillation energy $\varepsilon_2 = \omega_{ab} \neq 0$, or static for populations $|a\rangle\langle a|$ ($\varepsilon_2 = 0$).

To reveal oscillatory contributions in the DO and ED systems we have grouped all contributions into either oscillatory or static as shown in Fig. 2a. If we consider only the two main vibrational sub-states in DO, the 2DPE spectrum will have only ESE and GSB contributions, while ED additionally has ESA. As a function of t_2 , the DO system has 8 oscillatory and 8 static configurations, which organize into six peaks, while the ED system has only 4 oscillatory and 8 static contributions which give four peaks. The net result is that the diagonal peaks in the \mathbf{k}_I and cross-peaks in the \mathbf{k}_{II} signals are non-

oscillatory in the ED, while all peaks except the upper diagonal peak in \mathbf{k}_I are oscillatory in the DO. We thus find significant differences in oscillatory peaks between ED and DO systems.

An important additional parameter to consider is a phase of oscillation. Eq. (1) can be analytically integrated for $G_j(t_j) \propto \exp(-i\varepsilon_j t_j - \gamma_j t_j)$. For a single contribution S_n giving rise to a peak at $(\omega_1, \omega_3) = (\mp|\varepsilon_1|, \varepsilon_3)$ we shift the origin of (ω_1, ω_3) plot to the peak center by introducing the displacements $(\omega_1 + \varepsilon_1 = -s_1, \omega_3 - \varepsilon_3 = s_3)$ for the rephasing pathways, while $\omega_1 - \varepsilon_1 = s_1, \omega_3 - \varepsilon_3 = s_3$ for the nonrephasing). For $\gamma \approx \gamma_1 \approx \gamma_3$ we get the peak profile

$$S_n(s_3, t_2, s_1) = A_n L(s_1, s_3) e^{-\gamma_2 t_2} \cos(|\varepsilon_2| t_2 + \phi(s_1, s_3)), \quad (3)$$

where the lineshape and phase for the \mathbf{k}_I (upper sign) and \mathbf{k}_{II} (lower sign) signals are

$$L(s_1, s_3) = \frac{\sqrt{[\gamma^2 \pm s_1 s_3]^2 + \gamma^2 (s_3 \mp s_1)^2}}{(s_1^2 + \gamma^2)(s_3^2 + \gamma^2)}, \quad (4)$$

$$\phi(s_1, s_3) = \text{sgn}(\varepsilon_2) \arctan\left(\frac{\gamma(s_3 \mp s_1)}{(\mp s_1 s_3 - \gamma^2)}\right). \quad (5)$$

The phase ϕ and the full profile for $A_n = 1$ and $t_2 = 0$ are shown in Fig. 2c. The rephasing and non-rephasing configurations are obtained by flipping the direction of the s_1 axis. At the center of the peak ($s_1 = s_3 = 0$), we have and $\phi = 0$, leading to $S_n \propto \cos(|\varepsilon_2| t_2)$. However, for $(s_1 \neq 0, s_3 \neq 0)$ we find $S_n \propto \cos(|\varepsilon_2| t_2 + \phi(s_1, s_3))$ with $\phi(s_1, s_3) \neq 0$. Thus, *the displacement from the peak center determines the phase of the spectral oscillations*. Note that the sign of the phase ϕ is opposite for the peaks above ($\varepsilon_2 < 0$) and below ($\varepsilon_2 > 0$) the diagonal line, and this applies for all contributions.

The whole 2DPE spectrum is a sum of all relevant contributions. Assuming that all dephasings are similar, different contributions to the same peak will have the same spectral shape and they may be summed. We can then simplify the 2DPE plot by writing the signal as a sum of peaks $\sum_{i,j}$, which have static (from populations) and oscillatory (from coherences) parts:

$$S(\omega_3, t_2, \omega_1) = e^{-\gamma_2 t_2} \sum_{i,j} L_{ij}(\omega_1, \omega_3) \times [A_{ij}^p + A_{ij}^c \cdot \cos(|\omega_{ij}| t_2 + \phi_{ij}(\omega_1, \omega_3))]. \quad (6)$$

Here ω_{ij} is the characteristic oscillatory frequency of a peak (ij) , $A_{ij}^p(t_2)$ and $A_{ij}^c(t_2)$ are the real parts of orientationally-averaged prefactors of population and coherence (electronic or vibronic) contributions, respectively. The spectral lineshape is given by $L_{ij}(\omega_1, \omega_3)$. Here we clearly identify the oscillatory amplitude and its phase for a specific peak.

To apply this expression to our systems, we assume a typical situation where the spectrum of the laser pulses is tuned to the center of the absorption spectrum and the limited bandwidth selects the two strongest absorption peaks. In the 2DPE spectra two diagonal and two off-diagonal peaks for ED and DO are observed. Indices i

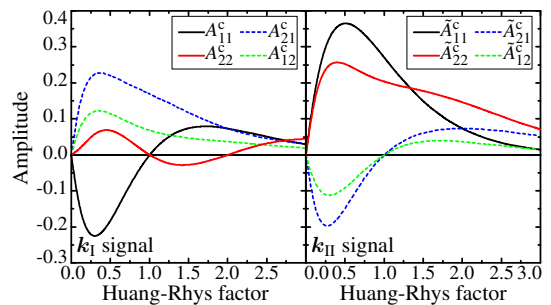


FIG. 3. The amplitudes of oscillatory peaks of 2D spectra of the DO model for \mathbf{k}_I and \mathbf{k}_{II} signal. Note that the negative amplitude denotes a phase shift of π of the oscillation.

and j in Eq. (6) run over the positions of the peaks and thus can be (1,1), (1,2), (2,1), and (2,2). For clarity we study the spectral dynamics with t_2 at the short delays, $t_2 \ll \gamma_2^{-1}$, and use notations A, L for the \mathbf{k}_I signal and \tilde{A}, \tilde{L} for the \mathbf{k}_{II} signal.

The transition dipole properties of the ED results in the picture where all static amplitudes of the ED are positive and $A_{11}^p = \tilde{A}_{11}^p, A_{22}^p = \tilde{A}_{22}^p, A_{12}^p = A_{21}^p = \tilde{A}_{21}^p = \tilde{A}_{12}^p$. The oscillatory amplitudes are equal: $A_{12}^c = A_{21}^c = \tilde{A}_{11}^c = \tilde{A}_{22}^c$. Such relationships are obtained by considering the all-parallel organization of polarization of incoming electric fields and neglecting the bi-exciton binding energy. The spectral beats with t_2 can thus only have the same phases in the \mathbf{k}_I or \mathbf{k}_{II} spectrum, when measured at peak centers. Additionally the oscillatory ESE and ESA parts in ED cancel each other if $\Delta = 0$ and their broadenings are equal. As these relationships do not depend on coupling J and transition dipole orientations, all ED systems should behave similarly. By studying the whole parameter space, it can also be shown that these relations hold for a hetero-dimer.

The amplitude-relationships, however, are different for the DO system. The amplitudes $A_{ij}^{(c)}$ of the oscillatory peaks are plotted in Fig. 3 as a function of the HR factor, where now we include all vibrational levels in the $|g_m\rangle$ and $|e_n\rangle$ ladders. For \mathbf{k}_I , the amplitudes A_{11}^c and A_{22}^c maintain the opposite sign when $HR < 2$ and are both positive when $2 < HR < 3$ (note that $A_{22}^c = 0$ when only two vibrational levels are considered in Fig. 2b). The oscillation amplitudes A_{11}^c and A_{22}^c change sign at $HR = 1$. Amplitudes A_{12}^c and A_{21}^c are always positive. Spectrum oscillations with t_2 for both diagonal peaks in the \mathbf{k}_{II} signal will be in-phase for the whole range of the HR factor. The same pattern holds for the 1-2 and 2-1 cross-peaks, which will oscillate in-phase, but will be of opposite phase compared to the diagonal peaks in the region of $HR < 1$. Note that the sign of amplitudes changes with the HR factor, since the overlap integral between vibrational wavefunctions can be both positive and negative. The amplitudes of static contributions are positive in the whole range of parameters and are identical for both \mathbf{k}_I and \mathbf{k}_{II} signals.

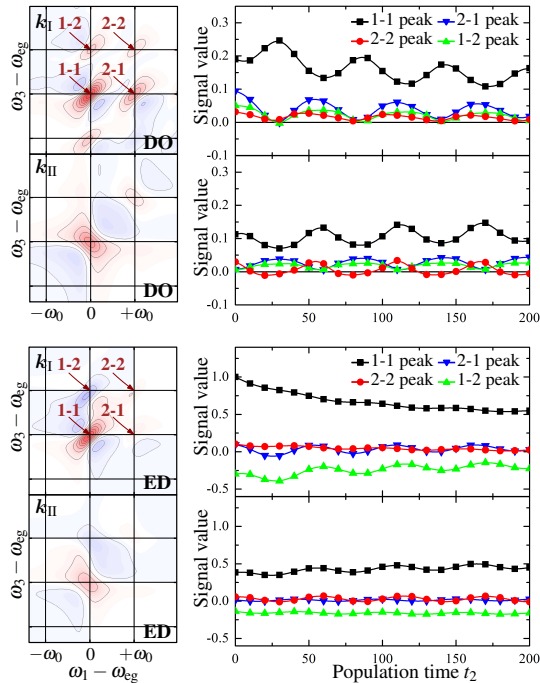


FIG. 4. 2DPE spectra and peak values of the DO and ED as the function of population time t_2 , of the k_I and k_{II} signals. Spectra are normalized to the maxima of the total spectra of the DO and ED.

We thus find very different behaviour of oscillatory peaks of DO and ED systems. The above analysis applies for the central positions of the peaks, which may be difficult to determine if the broadening is large. Note that the phase ϕ varies from $-\pi/2$ to $+\pi/2$ (Eq. (3) and Fig. 2c) when probing in the vicinity of the peak. However, $\phi = 0$ along the diagonal line for k_I and along the anti-diagonal line for k_{II} . These lines can thus be used as guidelines for reading phase relations of distinct peaks in the 2DPE spectrum. For instance, the two diagonal peaks can be calibrated by reading their amplitudes at the diagonal line, or the two opposite cross-peaks can be compared by drawing anti-diagonal lines.

The 2DPE spectra for both DO and ED systems calculated by including phenomenological relaxation and Gaussian laser pulse shapes^{14,15} are plotted in Fig. 4. The structure and the t_2 evolution of the spectra illustrate the dynamics discussed above and clearly shows the distinctive spectral properties of the vibronic vs. electronic system: (i) diagonal peaks in the k_I signal are oscillating in DO, but only exponentially decaying in ED (the oscillatory traces come from the overlapping tails of off-diagonal peaks), (ii) the relative amplitude of oscillations is much stronger in DO as compared to ED, where the ESA and ESE cancellation suppresses the oscillations, (iii) opposite oscillation phases are observed in DO, while all peaks oscillate in-phase in ED.

The up-to-date experiments are capable of creating broad-band pulses⁹. Thus, the overtones in DO can be excited and beats of $n\omega_0$ frequencies (n is integer) ob-

served. These may become important in the case of large HR factors. Such frequencies are absent in the ED system, since only one oscillatory frequency, equal to $2J$ is available.

The analysis presented in this article provides a clear physical picture of electronic and vibronic coherence beatings in 2DPE spectra. We are able to discriminate weakly damped electronic and vibronic coherent wavepackets in molecular systems based on fundamental theoretical considerations. Dynamics of diagonal peaks and cross-peaks as well as relative phase between them in the rephasing signal can now be classified for vibrational and excitonic systems as follows. (i) Static diagonal peaks and oscillatory off-diagonal peaks signify pure electronic coherences, not involved in energy transport. (ii) Oscillatory diagonal peaks in accord with off-diagonal peaks (0 or π phase relationships) signify vibronic origins. The oscillation phase is 0 for electronic coherences and 0 or π for vibronic coherences. These outcomes hold if the signal is probed at the very centers of the spectral resonances. The observed phase of the beatings varies as the signal is recorded away from the center of an oscillating peak.

Our results might be useful in analysis of recently observed beatings in molecular systems. For instance phase relations of the beatings detected at separate points in the vicinity of the same cross-peak of the photosynthetic LH2 complex¹⁶ might be the result of measurement away from the peak center (see Fig. 2b). The issue of probing away from the peak centers also applies to the opposite-phase beatings reported by Collini et al.⁷. Our analysis thus shows that the detailed phase relationships in the two dimensional spectra may be of critical importance. By helping to identify spectral beats in photosynthetic aggregates, the presented analysis should facilitate answering the question of importance of electronic coherences in excitonic energy transfer, its efficiency and robustness.

This research was funded by the European Social Fund under the Global Grant measure.

- ¹P. F. Tian, D. Keusters, Y. Suzaki, and W. S. Warren, *Science* **300**, 1553 (2003).
- ²X. Li, T. Zhang, C. N. Borca, and S. T. Cundiff, *Phys. Rev. Lett.* **96**, 057406 (2006).
- ³G. S. Engel, T. R. Calhoun, E. L. Read, T. K. Ahn, T. Mančal, Y. C. Cheng, R. E. Blankenship, and G. R. Fleming, *Nature* **446**, 782 (2007).
- ⁴E. Collini and G. D. Scholes, *Science* **323**, 369 (2009).
- ⁵F. Caruso, A. W. Chin, A. Datta, S. F. Huelga, and M. Plenio, *J. Chem. Phys.* **131**, 105106 (2009).
- ⁶P. Rebentrost, M. Mohseni, and A. A. Guzik, *J. Phys. Chem. B* **113**, 9942 (2009).
- ⁷E. Collini, C. Y. Wong, K. E. Wilk, P. M. G. Curmi, P. Brumer, and G. D. Scholes, *Nature* **463**, 644 (2010).
- ⁸A. Nemeth, F. Milota, T. Mančal, V. Lukeš, J. Hauer, H. F. Kauffmann, and J. Sperling, *J. Chem. Phys.* **132**, 184514 (2010).
- ⁹N. Christensson, F. Milota, J. Hauer, J. Sperling, O. Bixner, A. Nemeth, and H. F. Kauffmann, *J. Phys. Chem. B* **115**, 5383 (2011).
- ¹⁰D. B. Turner, K. E. Wilk, P. M. G. Curmi, and G. D. Scholes, *J. Phys. Chem. Lett.* **2**, 1904 (2011).

- ¹¹V. May and O. Kühn, *Charge and Energy Transfer Dynamics in Molecular Systems* (Wiley-VCH, 2011).
- ¹²S. Mukamel, *Principles of Nonlinear Optical Spectroscopy* (Oxford University Press, New York, 1995).
- ¹³H. van Amerongen, L. Valkunas, and R. van Grondelle, *Photosynthetic Excitons* (World Scientific, Singapore, 2000).
- ¹⁴D. Abramavicius, L. Valkunas, and S. Mukamel, *Europhys. Lett.* **80**, 17005 (2007).
- ¹⁵D. Abramavicius, V. Butkus, J. Bujokas, and L. Valkunas, *Chem. Phys.* **372**, 22 (2010).
- ¹⁶E. Harel and G. S. Engel, *Proc. Nat. Acad. Sci. USA* **109**, 706 (2012).